Progress In Electromagnetics Research C, Vol. 40, 243–256, 2013

ACCURATE MAGNETIC FLUX MEASUREMENTS IN ELECTROMAGNETIC RAIL LAUNCHERS

Roberto Ferrero, Mirko Marracci, and Bernardo Tellini*

Department of Energy, Systems, Land and Constructions, University of Pisa, Largo L. Lazzarino, Pisa I-56122, Italy

Abstract—This paper deals with the measurement of the magnetic flux generated by the armature of electromagnetic rail launchers linked with external pick-up loops. In particular we discuss possible methods to experimentally evaluate measurement uncertainty when the magnetic flux is obtained by numerical voltage integration. These methods aim at an approximate identification of the correlation among voltage samples introduced by the analog-to-digital converter, only based on the available measurements without requiring additional tests and instruments. An estimate of this correlation allows to better evaluate the overall measurement uncertainty, thus providing the applicability limits of the proposed inductive technique and contributing to a better understanding of the current and force distribution in the armature.

1. INTRODUCTION

The use of digital signal processing (DSP) algorithms to elaborate measured data in modern instrumentation is growing as digital instruments are becoming more accurate. The problem of a correct uncertainty evaluation of the results provided by these algorithms is therefore particularly important. A significant example is represented by numerical integration, which is involved in many common operations. This occurs, for example, when the rms or mean values of a signal need to be computed starting from its samples [1, 2] or when the Fourier spectrum is calculated via the Discrete Fourier Transform algorithm [3, 4].

Voltage signal integration can be usefully employed also to measure a time-varying magnetic flux linked to a circuit, from

Received 18 April 2013, Accepted 31 May 2013, Scheduled 3 June 2013

* Corresponding author: Bernardo Tellini (bernardo.tellini@ing.unipi.it).

the measurement of the induced voltage on that circuit. This technique was recently applied by the authors for characterization of magnetic materials via inductive methods to investigate magnetic accommodation of minor asymmetric loops [5] and to pulse current measurements on an electromagnetic rail launcher, with the aim of measuring the current distribution between the armature brushes [6–9]. In more detail, in the specific case of the rail launcher a set of pick-up loops was placed near the brushes and the voltage pulses induced on the loops were acquired; the integration of these signals provided the magnetic fluxes linked to the loops and from them the unknown brush currents could be reconstructed. In such application, a correct estimate of the flux uncertainty is essential to evaluate the uncertainty of the reconstructed currents and to identify the conditions in which this method can provide meaningful results.

Though the algorithm employed to integrate the voltage signal can be extremely simple (in its simplest version it is just a sum), the evaluation of the integrated signal uncertainty is not that simple [10, 11], e.g., because of the critical role of correlation among voltage samples in the uncertainty propagation through the integration algorithm [12–14]. In fact, when the number of samples involved in the integration is very high, a wrong estimate of the correlations among them might lead to a significant error in the uncertainty evaluation of the integrated signal. In this framework different approaches can be found in the literature. In some cases it is assumed that when the samples come from the same source as a temporal sequence they are strongly correlated and the correlation between them plays a fundamental role [13, 15], in other cases it is assumed that they can be considered to be statistically independent of each other [16].

Besides being important for the flux uncertainty evaluation, a correct correlation estimate is important also for the choice of the best analog-to-digital converter (ADC) for the acquisition of a particular voltage signal that needs to be integrated.

The aim of this paper is to provide valuable and convenient methods to estimate the uncertainty propagation through the integration algorithm, via an empirical evaluation of the correlation among voltage samples. This allows to better identify the applicability limits of numerical integration for magnetic flux measurements in electromagnetic rail launchers. The proposed methods are only based on the available measurements, without requiring additional tests and instruments. In Section 2 a theoretical background of the analyzed problem is reported. In Section 3 a theoretical analysis of the uncertainty propagation is presented and simple expressions taking into account the correlation are derived. Then, the proposed

methods to experimentally identify the correlation are tested on the electromagnetic launcher application described above and the results are reported in Section 4.

2. THEORETICAL BACKGROUND

The electromagnetic driving equation in a rail launcher can be easily derived from the two following Maxwell's equations:

$$\nabla \times E = -\mu \frac{\partial H}{\partial t} \tag{1}$$

$$\nabla \times H = \sigma E + \sigma \mu (v \times H) \tag{2}$$

where the term $\sigma\mu(v \times H)$ in the second equation represents the motional contribution due to the movement of the armature, being v the armature velocity. By combining the two equations, we obtain:

$$\nabla^2 H = \mu\sigma \frac{\partial H}{\partial t} + \mu\sigma(\nabla \times v \times H) \tag{3}$$

The nonlinear nature of the driving equation and the presence of multi-physic phenomena, such as plasma formation, ablation, velocity-skin effect require the use of very complex numerical models to develop accurate simulations, nowadays still not available. This makes the possibility to perform accurate measurements very important for validation and improvement of numerical models. On the other hand, due to the very critical environment the measurement itself is also a great challenge.

A critical issue is the accurate measurement of the current distribution in the rail-armature system to estimate the thrust force on the armature and the possible formation of ablation. In more detail, the force can be expressed as:

$$F = m_a a = \frac{\partial W_m}{\partial x} - F_d - F_a \tag{4}$$

where F_d and F_a are terms representing the drag force and forces due to possible ablation effects, while $W_m = Li^2/2$ is the magnetic energy.

Our approach to such a measurement task estimates the current distribution via an inductive method measuring the magnetic flux linked with proper pick-up loops. According to the Faraday-Lenz's law, the measured induced voltage is the derivative of the linked flux. Thus, the measurement chain implies the integration of the measured signal. Here, we present the results of an experimental analysis aimed at evaluating the measurement uncertainty when the magnetic flux is obtained by numerical voltage integration. Results show how the errors of the A/D converter and the correlation profile among the acquired

samples can play an important role in the estimation of the overall measurement uncertainty.

3. UNCERTAINTY PROPAGATION THROUGH INTEGRATION

The proposed measurement method is described in [8, 9] and is based on the use of external pick-up loops, magnetically coupled to the launcher circuit. The integration of the induced voltages along the loops provides the corresponding linked fluxes, which are linear combinations of the currents flowing in the armature brushes. If the mutual inductances between the loops and the launcher circuit are known, the currents flowing in the brushes can be calculated. The model reads as:

$$[\phi] = [M][i] \tag{5}$$

where $[i]$ is the vector of the unknown brush currents, $[\phi]$ the vector of the magnetic fluxes linked to the pick-up loops, and $[M]$ the mutual inductance matrix between the loops and the launcher circuit. The Faraday-Lenz's law implies:

$$[v] = -\frac{d}{dt}[\phi] \tag{6}$$

and $[\phi]$ is obtained by integration of the measured voltage. Let us consider a voltage signal $v(t)$ sampled with a sampling time T_s and let us suppose, without loss of generality, that both $v(t)$ and the corresponding flux $\phi(t)$ linked to the circuit are zero at $t = 0$. If the flux $\phi(nT_s) = \phi_n$ at the discrete time nT_s is calculated by numerical integration of the voltage samples $v_1, \ldots, v_n$ using the trapezoidal rule, the following expression for ϕ_n is obtained:

$$\phi_n = \phi_{n-1} + \frac{v_n + v_{n-1}}{2} T_s = \left(\frac{v_n}{2} + \sum_{i=1}^{n-1} v_i \right) T_s \tag{7}$$

If the signal $v(t)$ is smooth enough so that a constant-second-derivative approximation is valid in each sampling interval, an estimate of the integration error associated with this algorithm can be calculated and it is proportional to N^{-2}, being N the number of samples in the given time interval. In most practical conditions, the number of samples N is high enough to ensure that this error is negligible compared to other error or uncertainty sources, that will be discussed below. Therefore there is no need to employ more complex integration algorithms or try to compensate this error.

The most important uncertainty contribution on the flux ϕ_n is the propagation of the uncertainties of the voltage samples through the

integration algorithm. Let us consider again (7), here approximated for sake of simplicity by:

$$\phi_n = \sum_{i=1}^{n} v_i T_s \tag{8}$$

which is formally equivalent to rectangular numerical integration. Each measured sample v_i differs from the ideal voltage because of the non-ideal behavior of the ADC. Calling $u(v_i)$ the uncertainty of each voltage sample v_i, the resulting uncertainty of ϕ_n depends on how $u(v_i)$ propagates through the integration algorithm. This in turn depends on the random or non-random nature of the effects that underlie this uncertainty and their correlation among different samples.

Generally speaking, two uncertainty sources can be distinguished in a voltage measurement: the non-ideal transfer characteristic of the ADC and random noise including random analog noise at the ADC input stage and quantization noise. The former produces a systematic effect, though different for each voltage value and usually unknown; for this reason it is taken into account in the converter specifications by providing a general accuracy estimate. The latter, on the contrary, produces a random effect and in a first approximation it can be described as a white noise whose standard deviation is provided in the converter specifications or it can be easily measured. For what concerns the ADC accuracy, some correlation between samples close to each other is likely to be present. Thus the following general expression for uncertainty propagation should be employed to evaluate the flux uncertainty [12]:

$$u\left(\phi_n\right) = \sqrt{\sum_{i=1}^{n} \left(u^2\left(v_i\right) + \sum_{j=i+1}^{n} 2\rho_{ij} u\left(v_i\right) u\left(v_j\right) \right)} T_s \tag{9}$$

being ρ_{ij} the uncertainty correlation between the samples v_i and v_j.

For sake of simplicity let us suppose that the uncertainty $u(v)$ is constant for all samples. Thus, the two limit cases of (9) for uncorrelated random noise ($\rho_{ij} = 0$) or constant systematic contribution ($\rho_{ij} = 1$) are respectively:

$$\begin{aligned} u_{\text{ran}}\left(\phi_n\right) &= \sqrt{n} T_s u\left(v\right) \\ u_{\text{sys}}\left(\phi_n\right) &= n T_s u\left(v\right) \end{aligned} \tag{10}$$

On the other hand, for the intermediate case of a typical voltage measurement affected by both random and systematic effects, it is reasonable to assume that closer samples have a higher correlation than more distant ones. Thus, for an approximate estimate of the

correlation coefficients ρ_{ij} it is possible to define a constant correlation distance d and to assume that ρ linearly varies from 1 to 0 as the distance between the two samples goes from 0 to $d+1$. The following expression for the uncertainty of ϕ_n is then obtained:

$$u_{\rho,\mathrm{lin}}(\phi_n) = \begin{cases} \sqrt{n + \frac{n(n-1)(3d-n+2)}{3(d+1)}}\, T_s u(v) & n \le d+1 \\ \sqrt{n + nd - \frac{d(d+2)}{3}}\, T_s u(v) & n > d+1 \end{cases} \tag{11}$$

The uncertainty propagation (11) is compared to the two limit cases (10) in Fig. 1.

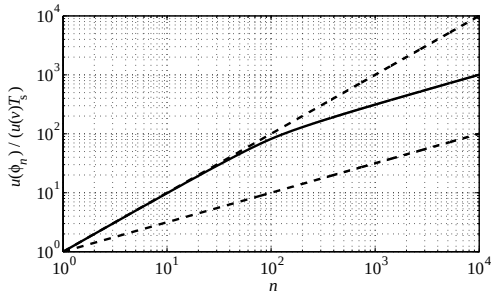

Figure 1. Propagations of the uncertainty $u(v)$ through integration according to (11) with $d = 100$ (solid line), compared to the limit cases (10) (dashed lines).

The expression in (11) shows that when samples close to each other are correlated, a further increase in the sampling frequency does not produce any uncertainty decrease. Thus it is possible to state that there is a practical maximum sampling frequency corresponding to the minimum achievable uncertainty. An evaluation of this limit is important for the choice of the converter, which usually implies a trade-off between high sampling frequency and low accuracy.

4. INTEGRATION OF RAIL LAUNCHER PULSE SIGNAL

The discussion presented in the previous section proved that a wrong estimate of the correlation among voltage samples in numerical integration can lead to significant under- or over-estimations of the flux uncertainty. This represents a significant problem in the launcher application described in the introduction because the flux uncertainty strongly affects the uncertainty of the brush currents, reconstructed from the flux measurements [7, 9].

In this section, possible methods to estimate the correlation among voltage samples are discussed and compared, applied to the rail launcher pulse signals. In more details, these methods aim at estimating the correlation distance d according to the uncertainty propagation (11) derived in the previous section. Different methods are presented, suitable to be applied in different conditions depending on the available measurements.

The experimental setup is composed of a 765 μF capacitor as energy source, with 10 kV maximum applicable voltage. This capacitor is connected through a coaxial cable to a rail launcher composed of two parallel rails and a moving armature with thin brushes that close the circuit between them; a set of pick-up loops is placed near the launcher and the induced voltages on the loops are measured. More details about this setup can be found in [8, 9]. The focus here is on the measurement of the magnetic flux linked to the external pick-up loops, obtained by integration of the induced voltages; however, the problem of voltage integration arises also for other current transducers, such as the Rogowski coil, which is one of the possible solutions adopted for the rail launcher current measurement [17].

A typical voltage pulse measured on a loop is shown in Fig. 2, together with the flux obtained by voltage integration. The voltage signals were acquired by a 14-channel 12-bit oscilloscope (Yokogawa DL750 ScopeCorder with 701250 analog voltage input module) with 10^7 samples-per-second sampling frequency, which is the maximum allowed by the instrument. Each channel has its own ADC, therefore the results provided by different channels are independent from each other.

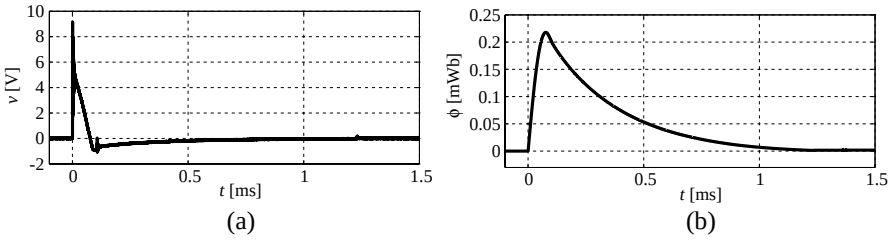

Figure 2. Typical pulse signals: (a) voltage and (b) flux.

Each pulse was simultaneously acquired by 4 oscilloscope channels and 20 pulses were repeated in proper conditions to ensure a good reproducibility of the results. The channel offset and noise for each signal were evaluated by acquiring 100 ms (10^6 samples) of zero-voltage signal before and after the pulse. The offset measurement is needed to

compensate it when integrating the signal; it was measured both before and after the useful signal to verify that its value did not significantly change during the whole observation time.

After having removed their offsets, all voltage signals were integrated in the time interval from 0 to 1.3 ms (assumed as the end of the transient), thus 80 flux measurements were obtained (20 for each channel). The final values at $t = 1.3\,\text{ms}$ are shown in Fig. 3. The choice of the end of the transient for this analysis is particularly useful because the true value of the flux is known to be zero for physical reasons (there is no more current producing a magnetic field).

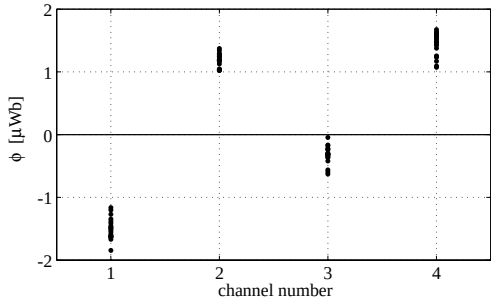

Figure 3. Final flux values at $t = 1.3\,\text{ms}$ for the 4 channels; 20 values are plotted for each channel.

From this figure it can be seen that the differences among the 20 fluxes of the same channel are much smaller than the differences among fluxes of different channels and the difference with respect to zero, meaning that systematic uncertainty sources introduced by the ADCs are dominant over the random effects due to both noise and a not perfect repeatability of the voltage pulse.

According to the oscilloscope specifications in the selected range ($\pm 10\,\text{V}$), the voltage measurement is characterized by a $\pm 100\,\text{mV}$ accuracy, while the least significant bit (LSB) amplitude is 13.33 mV. In order to estimate the noise level for each channel and each signal, the standard deviation of the voltage samples in the 100 ms before and after the pulse ($2 \cdot 10^6$ samples) was calculated and it resulted to be about 10 mV for all signals and all channels. Since there is no reason to assume any correlation among noise on different samples, the uncertainty $u_{\text{noise}}(v)$ propagates through the integration algorithm according to the first expression in (10):

$$u_{\text{noise}}(\phi_n) = \sqrt{n} T_s u_{\text{noise}}(v) \tag{12}$$

leading to $u_{\text{noise}}(\phi) = 0.11\,\mu\text{Wb}$ at $t = 1.3\,\text{ms}$, which is similar to the experimental standard deviations of the 20 measurements of

each channel shown in Fig. 3, that vary from 0.11 μWb to 0.18 μWb depending on the channel.

On the other hand, as far as the ADC accuracy is considered, the equivalent uncertainty $u_{\mathrm{acc}}(v)$ can be evaluated assuming a rectangular probability distribution and thus it results $u_{\mathrm{acc}}(v) = 100\,\mathrm{mV}/\sqrt{3} = 57.7\,\mathrm{mV}$. For the propagation of this uncertainty the expression in (11) can be used:

$$u_{\mathrm{acc}}(\phi_n) = \begin{cases} \sqrt{n + \frac{n(n-1)(3d-n+2)}{3(d+1)}}\, T_s u_{\mathrm{acc}}(v) & n \le d+1 \\ \sqrt{n + nd - \frac{d(d+2)}{3}}\, T_s u_{\mathrm{acc}}(v) & n > d+1 \end{cases} \tag{13}$$

thus the distance d over which the voltage samples are correlated needs to be evaluated.

A possible approach for this evaluation is to undersample the voltage signals and recalculate the fluxes starting from these undersampled signals. In particular, being the new sampling time $T_s^* = kT_s$ (with k integer value), the variation of the final flux value vs. k can be analyzed. This is shown in Fig. 4(a) for a single signal. If the systematic uncertainty sources acting on k consecutive samples are completely (or highly) correlated to each other, no difference should be seen in the final flux value when the voltage signal is undersampled by a factor k, except for an increased effect of noise propagation described by:

$$u_{\mathrm{noise}}(\phi_{\mathrm{undersampled}}) = \sqrt{k}\, u_{\mathrm{noise}}(\phi_{\mathrm{original}}) \tag{14}$$

In this case, the flux variations are greater than what expected from the increased noise effect according to (14) even for very small values

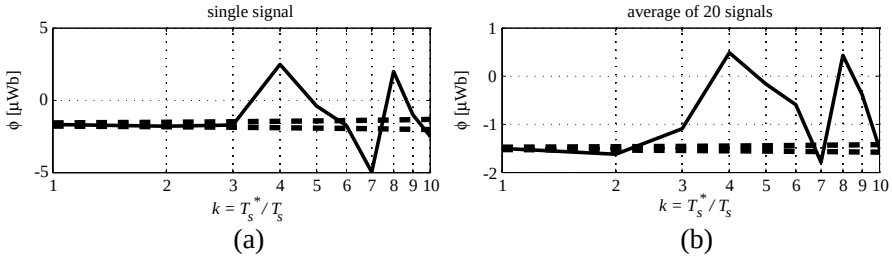

Figure 4. Final flux values at $t = 1.3\,\mathrm{ms}$ (solid lines) when the voltage signals are sampled with a sampling time $T_s^* = kT_s$, compared to the expected uncertainty of the flux values due to noise propagation alone (dashed lines) calculated according to (14). (a) Undersampling of a single signal. (a) Average of 20 undersampled signals acquired by the same channel.

of k. Therefore it seems that only very few samples are correlated (about 3).

It is worth to note that the main spectral components of the voltage pulses are in the range from 0.5 kHz to 10 kHz; although higher frequencies are also present in the spectrum, their amplitudes decrease vs. frequency and over 100 kHz they are below both the LSB value and the noise level of the employed oscilloscope. This means that the signal can be undersampled with an undersampling factor up to 50 (starting from a 10^7 samples-per-second sampling frequency) without the appearance of aliasing effects, thus the above analysis is justified.

The advantage of this approach is that it requires only one signal and thus it can be applied when it is not possible to acquire repeatable signals several times. However, if several signals with good repeatability are available as in this case, the above analysis can be repeated considering the average of all the signals acquired by the same channel, as shown in Fig. 4(b). This allows to better recognize the random nature of the flux variations vs. k. In fact, if they are random, the average of 20 signals decreases the standard deviation by $\sqrt{20}$, whereas the standard deviation would not be decreased if a systematic contribution were present. Also this analysis seems to confirm the results already obtained.

To further verify these results, the standard deviation of all channel fluxes can be analyzed. Fig. 5(a) shows the expected final flux uncertainty as a function of the correlation distance d calculated according to (13). It can be seen that the value corresponding to the experimental standard deviation (1.2 μWb) is reached for d between 2 and 3, confirming that at most 3 or 4 samples are correlated. As a final confirmation, the standard deviation of all the final flux values can be analyzed vs. the undersampling factor k; it is expected to remain

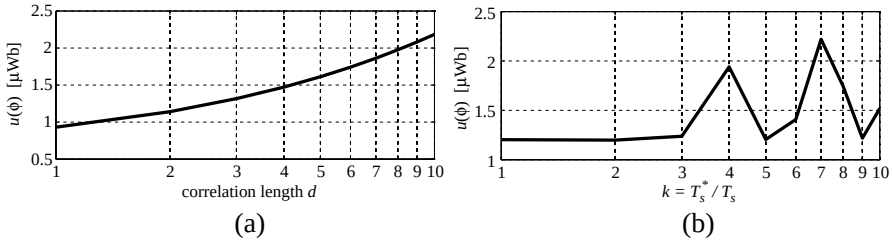

Figure 5. Uncertainty of the final flux values due to the propagation of systematic uncertainty sources. (a) Expected uncertainty vs. the correlation length d calculated according to (13). (b) Standard deviation of the experimental data vs. the undersampling factor k.

approximately constant for k smaller than d because of the correlation among samples, whereas it increases for higher k. This is shown in Fig. 5(b); it can be seen that the standard deviation appears to be approximately constant for k up to 3.

This last method provides the best estimate of the flux uncertainty because it can directly evaluate the systematic effects on each channel, based on the comparison among measurements obtained by several independent channels. However, such approach is often unfeasible because of the impossibility to acquire the same signal by several channels simultaneously or the impossibility to create repeatable signals. This method was employed here to verify that the analysis based on undersampling a single signal can provide sufficiently accurate results and it allows to obtain an estimate of the correlation of systematic uncertainty sources even when only one signal is available.

In conclusion, it seems that the employed sampling frequency is close to the practical maximum value over which no further decrease of the flux uncertainty is possible because of correlation. Therefore the choice of this converter should represent a good trade-off between high sampling frequency and low accuracy.

To verify this statement and to test the proposed methods also when some correlation among samples is actually present, the above results are compared to the results obtained by acquiring the same signals using a 8-bit oscilloscope (LeCroy WavePro 725Zi) with 10^9 samples-per-second sampling frequency. In this case the number of samples is 100 times greater, but the accuracy is worse (242 mV instead of 100 mV). The standard deviations of the 20 final flux values of the same channel are about 1.9 µWb, whereas the global standard deviation of all signals is 3.3 µWb.

The effects of undersampling are shown in Figs. 6 and 7, with the same meaning of Figs. 4 and 5. They all show a correlation distance d between 200 and 400. Considering that the sampling frequency is 100 times the previous sampling frequency, the d values obtained with the two oscilloscopes correspond approximately to the same time interval. Although it is in general meaningless to compare correlation distances of signals acquired by different ADCs, the agreement between the two results can be justified in this case by the similar accuracy of the two converters. In conclusion, the increase of the sampling frequency has not produced a decrease in the final flux uncertainty; on the contrary, the flux uncertainty has increased because of the worse converter accuracy.

As a final remark, it can be noted that the physical constraint of zero flux at the end of the transient can be employed to obtain a better estimate of the flux value during the whole transient and

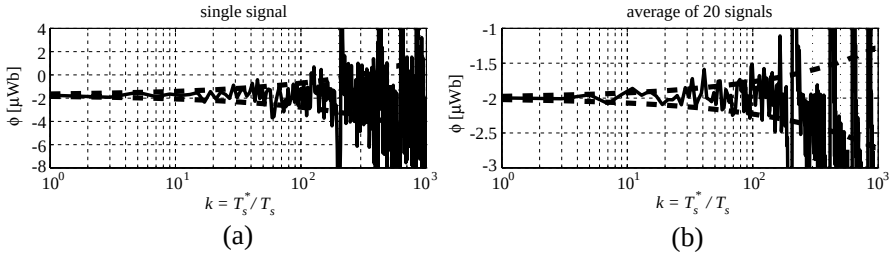

Figure 6. Final flux values at $t = 1.3$ ms (solid lines) when the voltage signals are sampled with a sampling time $T_s^* = kT_s$, compared to the expected uncertainty of the flux values due to noise propagation alone (dashed lines) calculated according to (14). (a) Undersampling of a single signal. (b) Average of 20 undersampled signals acquired by the same channel.

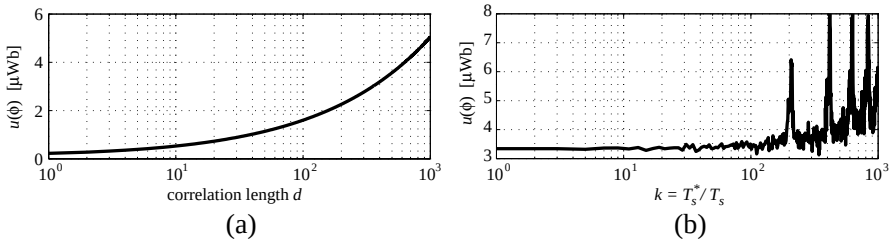

Figure 7. Uncertainty of the final flux values due to the propagation of systematic uncertainty sources. (a) Expected uncertainty vs. the correlation length d calculated according to (13). (b) Standard deviation of the experimental data vs. the undersampling factor k.

decrease its uncertainty. In fact the flux can be calculated also integrating the voltage signal backwards from the end of the transient. Having two different flux values, $\phi_{n,\text{for}}$ and $\phi_{n,\text{back}}$, each one with its own uncertainty, it is then possible to calculate a weighted average according to the well known formula:

$$\phi_n = \frac{1}{\frac{1}{u^2\left(\phi_{n,\text{for}}\right)} + \frac{1}{u^2\left(\phi_{n,\text{back}}\right)}} \left(\frac{\phi_{n,\text{for}}}{u^2\left(\phi_{n,\text{for}}\right)} + \frac{\phi_{n,\text{back}}}{u^2\left(\phi_{n,\text{back}}\right)} \right) \tag{15}$$

whose uncertainty is:

$$u\left(\phi_n\right) = \sqrt{\frac{1}{\frac{1}{u^2\left(\phi_{n,\text{for}}\right)} + \frac{1}{u^2\left(\phi_{n,\text{back}}\right)}}} \tag{16}$$

where:

$$u\left(\phi_{n,\text{back}}\right) = u\left(\phi_{N-n+1,\text{for}}\right) \tag{17}$$

5. CONCLUSIONS

The problem of uncertainty propagation through numerical integration of voltage signals was discussed, applied to magnetic flux measurements in electromagnetic rail launchers. A correct evaluation of the overall flux measurement uncertainty is important to provide the applicability limits of the proposed inductive technique aimed at evaluating the current and force distribution in the rail launchers armature.

In this problem the correlation among samples due to systematic uncertainty sources introduced by the ADC plays a very important role. Therefore, possible approaches to estimate this correlation were proposed and compared. The applicability of each approach was discussed, depending on the availability of repeatable signals and independent measurements.

All the proposed methods provided results in agreement with each other, both in case of negligible correlation and in case of significant correlation among a great number of samples.

REFERENCES

1. Novotny, M. and M. Sedlacek, "RMS value measurement based on classical and modified digital signal processing algorithms," *Measurement*, Vol. 41, 236–250, 2008.
2. Novotny, M., D. Slepicka, and M. Sedlacek, "Uncertainty analysis of the RMS value and phase in the frequency domain by noncoherent sampling," *IEEE Trans. Instrum. Meas.*, Vol. 56, No. 3, 983–989, 2007.
3. Xi, J. and J. F. Chicharo, "A new algorithm for improving the accuracy of periodic signal analysis," *IEEE Trans. Instrum. Meas.*, Vol. 45, No. 4, 827–830, 1996.
4. Betta, G., C. Liguori, and A. Pietrosanto, "Propagation of uncertainty in a discrete Fourier transform algorithm," *Measurement*, Vol. 27, 231–239, 2000.
5. Attivissimo, F., N. Giaquinto, M. Marracci, and B. Tellini, "Effect and compensation of ADC nonlinearity on magnetic accommodation measurements," *Measurement*, Vol. 46, No. 3, 1340–1348, 2013.
6. Ferrero, R., M. Marracci, and B. Tellini, "Characterization of inductance gradient and current distribution in electromagnetic

launchers," *IEEE Trans. Instrum. Meas.*, Vol. 60, No. 5, 1795–1801, 2011.

7. Ferrero, R., M. Marracci, and B. Tellini, "Uncertainty analysis of local and integral methods for current distribution measurements," *IEEE Trans. Instrum. Meas.*, Vol. 62, No. 1, 177–184, 2013.
8. Ferrero, R., M. Marracci, and B. Tellini, "Dynamic experiments of current distribution in rail launcher multi-brush armatures," *Proc. I²MTC*, 1–5, Graz, Austria, May 13–16, 2012.
9. Ferrero, R., M. Marracci, and B. Tellini, "Current distribution measurements in rail launcher multibrush armatures during launch," *IEEE Trans. Instrum. Meas.*, Vol. 62, No. 5, 1138–1144, 2013.
10. Cordero, R. R., G. Seckmeyer, D. Pissulla, and F. Labbe, "Uncertainty of experimental integrals: Application to the UV index calculation," *Metrologia*, Vol. 45, 1–10, 2008.
11. Edwards, T. S., "Effects of aliasing on numerical integration," *Mechanical Systems and Signal Processing*, Vol. 21, 165–176, 2007.
12. BIPM JCGM 100:2008, "Evaluation of measurement data — Guide to the expression of uncertainty in measurement," GUM 1995 with Minor Corrections, 2008.
13. Pogliano, U., "Traceability of electrical quantities obtained by sampling," *Measurement*, Vol. 42, 1439–1442, 2009.
14. Pogliano, U., "Evaluation of the uncertainties in the measurement of distorted power by means of the IEN sampling system," *IEEE Trans. Instrum. Meas.*, Vol. 55, No. 2, 620–624, 2006.
15. Nuccio, S. and C. Spataro, "Approaches to evaluate the virtual instrumentation measurement uncertainties," *IEEE Trans. Instrum. Meas.*, Vol. 51, No. 6, 1347–1352, 2002.
16. Locci, N., C. Muscas, and E. Ghiani, "Evaluation of uncertainty in measurements based on digitalized data," *Measurement*, Vol. 32, 265–272, 2002.
17. Ferrero, R., M. Marracci, and B. Tellini, "Analytical study of impulse current measuring shunts with cage configuration," *IEEE Trans. Instrum. Meas.*, Vol. 61, No. 5, 1260–1267, 2012.